

Theoretical study of shear-modulus instabilities in the alkali metals under hydrostatic pressure

Frederick Milstein and Daniel J. Rasky*

Departments of Materials and Mechanical Engineering, University of California, Santa Barbara, California 93106

(Received 23 February 1996)

The elastic stability of the bcc and fcc alkali metals is studied theoretically over wide ranges of hydrostatic pressure P . A pseudopotential model is employed to compute the variations of the bulk moduli κ and shear moduli μ and μ' , as well as the differences between the Gibbs energies of the two structures. Stability is assessed according to the criteria of Hill and Milstein, i.e., $\kappa(P) > 0$, $\mu(P) > 0$, and $\mu'(P) > 0$. In compression, the stability ranges of both phases are controlled primarily by the shear modulus μ , and high pressure bcc \rightarrow fcc transitions in K, Rb, and Cs are found to be associated with the vanishing of this modulus. The "interplay" between the ranges of elastic stability and thermodynamic phase equilibrium (at 0 K) is also studied. [S0163-1829(96)05129-6]

I. INTRODUCTION

Rasky and Milstein¹ have derived formulas for computing the elastic moduli of cubic metals, that are described by pseudopotential models, under axial load. Here these formulas are used to compute the elastic moduli of the alkali metals in their bcc and fcc configurations under hydrostatic pressure, and the computational results are used to evaluate the pressure dependency of the elastic stability of these structures. Stability is assessed according to the criteria developed by Hill and Milstein²⁻⁴ which, for a cubic crystal under a constant hydrostatic pressure P , may be expressed as

$$\kappa(P) > 0, \quad \mu(P) > 0, \quad \text{and} \quad \mu'(P) > 0, \quad (1)$$

where κ is the bulk modulus and μ and μ' are the shear moduli in the relation between the cubic axes components of the Cauchy stress increment $\delta\sigma_{ij}$ and the rotationless strain increment ε_{ij} (evaluated relative to the current configuration under pressure P). While, in principle, the vanishing of any one of the three elastic moduli (κ , μ , or μ') may induce an instability in a cubic crystal under hydrostatic pressure, we have found that it is specifically the shear modulus μ that controls the domains of elastic stability of the alkali metals under compression in both their bcc and fcc configurations (with the possible exception of Li at very high pressures). We also determine the difference between the Gibbs energy of the bcc and fcc structures under pressure (at 0 K) and thus are able to study the "interplay" of the ranges of elastic stability and thermodynamic phase equilibrium.

The alkali metals exhibit seemingly diverse experimental behavior. For example, at low temperatures, the heavier metals Cs, Rb, and K are bcc while Na and Li are in close-packed structures that are similar to fcc with periodic stacking faults;⁵ such close-packed structures evidently differ little in energy from the fcc phase. Indeed, cold working of Li below 75 K produces fcc.⁵ Under pressure, Cs, Rb, and K undergo bcc \rightarrow fcc transitions, with the transition pressure greatest for K and least for Cs;⁵ also, experimentally, Na transforms from a close-packed structure to bcc at a relatively low pressure, and the bcc and close-packed structures coexist over a large range of pressure.^{5,6} Here, from a theo-

retical viewpoint, we show that the bcc \rightarrow fcc transformations in the heavier alkali metals are associated with the vanishing of the shear modulus μ of the bcc structure (or μ_B) and the simultaneous growth of the shear modulus μ of the fcc structure (or μ_F), from negative or "weakly positive" to "strongly positive." For Na, however, both the bcc and fcc structures exhibit elastic stability over wide ranges of compression in the region of the transition between the bcc and close-packed structures, in accord with the experimentally observed "sluggishness" in this transition. Finally, each alkali metal has a qualitatively similar response to hydrostatic loading, but the respective curves of shear moduli and Gibbs energy difference are systematically shifted "toward the region of higher compression" in passing through the series from Cs to Li. The experimentally observed "diversity" in the low-temperature, pressure-dependent, behavior of the alkali metals may be understood as a natural consequence of this "shifting."

II. STABILITY CRITERIA

Milstein and Hill³ have employed the principles of bifurcation analyses for general materials in the determination of stability criteria for cubic crystals subjected to hydrostatic loading. The analyses are carried out in a manner equivalent to Hill (Ref. 7, Chap. III, Sec. C2) but without recourse to the general mathematical apparatus for handling follower loadings. Milstein and Hill's treatment of crystal stability is rigorous and complete; i.e., (a) the loading environment is fully specified, to sufficient order and in both its active and passive modes, and (b) the potential energy of the system as a whole is examined in all the nearby, possibly inhomogeneous, configurations allowed by the kinematic constraints, if any. Under a hydrostatic pressure that does not vary during any departure from a considered configuration of equilibrium, elastic stability is guaranteed if³

$$\begin{aligned} &\kappa(\varepsilon_{11} + \varepsilon_{22} + \varepsilon_{33})^2 + \frac{2}{3} \mu [(\varepsilon_{11} - \varepsilon_{22})^2 + \cdot + \cdot] \\ &+ 4\mu'(\varepsilon_{12}^2 + \cdot + \cdot) > 0, \end{aligned} \quad (2)$$

where ε_{ij} denotes the Eulerian strain rate in components on the cubic axes. Since the three terms are independently variable, the necessary and sufficient conditions for stability are the simultaneous satisfaction of the inequalities of relations (1). Milstein and Hill³ identified the primary eigenstates and corresponding eigensolutions η_{ij} associated with loss of stability on a fundamental path at a pressure $P=Q$ as follows.

(i) $\kappa(Q)=0$, $\mu(Q)>0$, $\mu'(Q)>0$ with eigensolution $\eta_{11}=\eta_{22}=\eta_{33}\neq 0$; $\eta_{12}=\eta_{23}=\eta_{31}=0$ (the eigenmode is necessarily homogeneous and purely volumetric, coincident with $dP/dV=0$, where V is the volume of the crystal).

(ii) $\mu(Q)=0$, $\kappa(Q)>0$, $\mu'(Q)>0$ with solutions such that $\eta_{11}+\eta_{22}+\eta_{33}=0$; $\eta_{12}=\eta_{23}=\eta_{31}=0$ (the uniform eigenmodes make the lattice orthorhombic, or possibly tetragonal, without varying the cell volume).

(iii) $\mu'(Q)=0$, $\kappa(Q)>0$, $\mu(Q)>0$ with solutions such that $\eta_{11}=\eta_{22}=\eta_{33}=0$; any ratios $\eta_{12}:\eta_{23}:\eta_{31}$ (the uniform eigenmodes distort the lattice without varying the lengths of the cell edges).

It is important to distinguish between this treatment of stability and the ‘‘notional concept’’ introduced by Born, and variously implemented by later writers on crystal elasticity (see, e.g., Refs. 8–10). In pioneering work, Born and his co-workers^{11–13} took the ‘‘positive definiteness’’ of the matrix of elastic moduli c_{rs} (the values of which vary with crystal deformation) to be synonymous with stability; for cubic crystals under hydrostatic pressure Born’s criterion yields

$$c_{11}+2c_{12}>0, \quad c_{11}-c_{12}>0, \quad \text{and} \quad c_{44}>0. \quad (3)$$

However, as first noted by Hill,¹⁴ and elaborated by Hill and Milstein,² Born’s criterion [and hence relations (3)] inadequately treats the effects of external loading upon the assessment of stability. It follows, in general, that theoretical ‘‘ranges of stability’’ computed via Born’s criterion depend upon the choice of parameters used to define strain in a crystal under load, and thus such ranges do not represent intrinsic measures of crystal strength or stability. (There are some exceptions,² but none occur for hydrostatic loading.) We review these considerations briefly in the following paragraphs as a prelude to the present work.

Presume that the elastic stability of a homogeneously deformed crystal (under load) is to be tested by allowing the crystal to undergo arbitrary δ departures from its considered state of equilibrium. Elastic stability prevails if the combined incremental changes of internal energy $\delta\omega$ and external work done by the surroundings δu are positive for all possible δ departures, i.e., $\delta\omega-\delta u>0$ for stability. The internal energy ω per unit reference volume of a homogeneously deformed, simple crystal may be written, in principle, as a function of six generalized coordinates q_r ($r=1, \dots, 6$) that are used to specify crystal geometry. The change in internal energy during any test departure is then $\delta\omega=p_r\delta q_r+1/2c_{rs}\delta q_r\delta q_s+\dots$ (summation convention, $r, s=1, \dots, 6$), where $p_r=\partial\omega/\partial q_r$, $c_{rs}=\partial^2\omega/\partial q_r\partial q_s$, and the derivatives are to be evaluated for the crystal in its current state, under equilibrium loading (i.e., before any δ departure). Likewise the increment of external work per unit reference volume δu during a δ departure is expressible as $\delta u=p_r\delta q_r+1/2k_{rs}\delta q_r\delta q_s+\dots$, where the coefficients k_{rs}

depend on the test configuration and the choice of variables q_r .² The criterion for stability, to second order in the δq_r , is then

$$(c_{rs}-k_{rs})\delta q_r\delta q_s>0, \quad (4)$$

for arbitrary sets $\{\delta q_r\}$, when not all $\delta q_r=0$. [Relations (3), of course, follow from the incomplete notional concept $c_{rs}\delta q_r\delta q_s>0$.] In general, (a) the quantities p_r and c_{rs} are calculable as functions of the q_r for various choices of the q_r and models of atomic bonding (the literature contains many examples), (b) ‘‘the set of p_r can be related to the Cauchy tractions on the crystal, but the connection is rarely simple’’² (except, e.g., in loadings of simple crystals coincident with crystallographic symmetry axes), and (c) ‘‘the loading in laboratory experiments is usually frame dependent and the work is affected also by rotation of the specimen; the loads ‘‘follow’’ the material during any disturbance; they may, in addition, be deformation sensitive and so become different in kind from those in the state of equilibrium whose stability is under test . . . the increment δu of external work must be specified objectively to second order, like the increment $\delta\omega$ of internal energy.’’²

For a loading environment consisting of a uniformly pressurized fluid, with the apparatus designed so that the pressure P does not vary during a δ departure from a primary configuration of equilibrium, the k_{rs} are readily evaluated. In particular, if the crystal is cubic on the primary path, and the q_r are the components of the Green strain tensor (which was always employed by the Born school), then $k_{11}=P/\lambda$, $k_{12}=-P/\lambda$, and $k_{44}=P/\lambda$, and the stability criterion, relations (4), becomes

$$c_{11}+2c_{12}+P/\lambda>0, \quad c_{11}-c_{12}-2P/\lambda>0,$$

and

$$c_{44}-P/\lambda>0, \quad (5)$$

for the considered loading environment, as shown by Hill and Milstein.² The all-round stretch λ is the crystal lattice parameter divided by its value at $P=0$; the k_{rs} have the same symmetry as the c_{rs} . Hill and Milstein^{2,3} also showed that

$$\kappa=\lambda/3(c_{11}+2c_{12})+P/3, \quad \mu=\lambda/2(c_{11}-c_{12})-P,$$

and

$$\mu'=\lambda c_{44}-P, \quad (6)$$

so the respective inequalities of relations (5) are in fact equivalent to those of relations (1).

In summary, elastic stability under load is ‘‘machine dependent’’ and thus a rational attempt to assess the stability of a crystal at finite strain must incorporate the behavior of the machine; i.e., the behavior of the loading environment during a δ departure from a given crystallographic configuration must be specified and included in the analysis. The apparent onset of an instability in a crystal under load, according to the Born criterion, will depend upon one’s choice of moduli

(i.e., the geometric parameters q_r used in defining the moduli). Although application of the Born criterion with a particular choice of moduli may be considered as equivalent to the specification of “a particular machine,” the actual connection is rarely obvious or simple. The stability criteria [relations (1)] employed in the present study are correct and rigorous for a machine that applies a hydrostatic pressure *that remains constant and hydrostatic* during the initial departure from a cubic configuration (to possibly a noncubic configuration) at the onset of instability. These criteria are also the conditions ensuring all real (nonimaginary) elastic waves or long-wavelength phonons, as stated in general terms, for example, in Eq. (3.40) of Wallace’s book.¹⁵ Were the crystallographic departure to cause the loading to depart incrementally from its considered mode (e.g., a departure from cubic to tetragonal might induce a nonhydrostatic component of stress in some pressure-producing systems), the criteria would need to be modified to account for this “machine-dependent” behavior.

Milstein and Hill^{3,4} determined the domains of elastic stability for the entire family of Morse-function cubic crystals (fcc, bcc, and sc), over wide ranges of pressure. Their work clearly demonstrated that relations (3) are not only incorrect (under nonzero pressure) in principle, but they yield large discrepancies in computed “stability” ranges when compared with relations (1). (It is interesting to note, however, that for all bcc and fcc Morse-function crystals that are stable at zero pressure, the bulk and shear moduli increased monotonically with increasing pressure,^{3,4} unlike the present pseudopotential-based computations.)

III. COMPUTATIONAL PROCEDURE

In pseudopotential theory the binding energy per atom, E_{bind} may be written as a sum of a real-space part, $E_{\text{bind}}^r = E_v(\Omega) + \sum_{\mathbf{r}} E_r(\mathbf{r}, \Omega)$, and a reciprocal space part, $E_{\text{bind}}^q = \sum_{\mathbf{q}} E_q(\mathbf{q}, \Omega)$. The summations are over atomic positions \mathbf{r} and reciprocal-lattice vectors \mathbf{q} ; both summations depend on crystal structure (i.e., the geometric arrangement of atoms and the level of strain) and on the atomic volume Ω . In an orthorhombic crystallographic configuration, following Rasky and Milstein,¹ the Cauchy stresses are

$$\sigma_s = \frac{\alpha_s}{\Omega} \frac{\partial}{\partial a_s} (E_{\text{bind}}^r + E_{\text{bind}}^q)$$

and (strain-dependent) elastic moduli are conveniently defined as

$$C_{rs} \equiv \frac{\alpha_r \alpha_s}{\Omega} \frac{\partial^2}{\partial a_r \partial a_s} (E_{\text{bind}}^r + E_{\text{bind}}^q),$$

where the parameters a_1 , a_2 , and a_3 are the principal edges of the conventional crystallographic cell and a_4 , a_5 , and a_6 are their included angles; $\alpha_s = a_s$ if $s=1,2,3$ and $\alpha_s=1$ if $s=4,5,6$. For $s=1,2,3$, the σ_s are axial stresses acting parallel to the s th cell edge and for $s=4,5,6$ the σ_s are shear stresses; here cubic crystal symmetry requires all shear stresses on the faces of the cell to vanish and axial stresses $\sigma_1 = \sigma_2 = \sigma_3 = -P$. The pressure and C_{rs} are computed with the analytic formula derived in Ref. 1 [see Eqs. (A19), (A21), (A36), and (A37)]; these formulas are suitable for use with

general pseudopotential models of the type described above. The bulk and shear moduli are, in turn, computed from the relations

$$\kappa = \frac{1}{3} (C_{11} + 2C_{12} + 2P),$$

$$\mu = \frac{1}{2} (C_{11} - C_{12} - P),$$

and

$$\mu' = C_{44} - P, \quad (7)$$

which are equivalent to Eqs. (44) in Hill and Milstein.² [Equations (7) yield the same respective values of κ , μ , and μ' as Eqs. (6), of course. The apparent difference in the explicit P terms is owing to the different choices of strain variables in the definitions of the c_{rs} and C_{rs} , as mentioned briefly in Sec. II; see Refs. 2–4 for further discussion.]

In the present work, a two-parameter Heine-Abarenkov local model potential¹⁶ with the Taylor dielectric function¹⁷ were used in the description of atomic binding.¹⁸ In some of our computations a Born-Mayer repulsive interaction was also included to model d -band repulsion between near neighbors. The model is described explicitly in Ref. 1. We certainly are aware of more sophisticated models for computing binding energies of the alkali metals. However, owing to the relative complexity of the formulas for computing *elastic moduli* of crystals *under load* (see the Appendix in Ref. 1), we have selected the pseudopotential approach for this study. Furthermore, with but two adjustable parameters (i.e., ionic radius and well depth, which were determined for each of the alkali metals in Ref. 1), the model yields excellent agreement with experimental binding energies, atomic volumes, second- and third-order elastic moduli, and pressure-volume relations.¹ Also, we are aware of lithium’s known departure from “free-electron behavior,” which would be expected to cause greater discrepancies between theory and experiment in the case of Li than in the remaining alkali metals (and indeed that tendency is observed). Nevertheless, Li is included in the present study, both for the “purpose of completion” and because the theoretical mechanical response of Li at moderate pressures is in reasonably good agreement with experiment, as seen in Tables I and II and in Fig. 1 of Ref. 1.

IV. RESULTS AND DISCUSSION

Computations were made of the pressure, the bulk and shear moduli, and the associated domains of stability of the bcc and fcc configurations of each alkali metal (Li, Na, K, Rb, and Cs) over extensive ranges of hydrostatic compression and expansion. The results for compression are shown in Figs. 1(a)–1(e) and for expansion in Figs. 2(a)–2(e); numerical values of particular interest are tabulated in Table I. The stretch λ is of course related to the atomic volume Ω by $\lambda^3 = \Omega/\Omega_0$ where Ω_0 is the atomic volume in the unstressed state. While hydrostatic expansion is difficult to achieve in a controlled experiment, this mode is nonetheless of interest since, as is well known, states of pure hydrostatic tension can be approached locally near cracks and other stress raisers.³ In these figures, we observe the following *general* behaviors.

(1) At zero pressure ($\lambda=1$), all of the bcc and fcc bulk and

TABLE I. Theoretical values of pressure P and stretch λ at particular “states of interest” in Figs. 1–4 and structures with elastic stability and lower Gibbs energy. The particular states occur at the following stretch values: $\lambda = \Lambda_{\kappa}$ (or $\Lambda_{\kappa F}$ and $\Lambda_{\mu B(R)}$ for Li), where stability is lost in hydrostatic tension; $\lambda = \Lambda_{\mu B(M)}$ and $\lambda = \Lambda_{\mu B(L)}$ where, respectively, stability of the bcc structure is lost and regained under increasing compression; $\lambda = \Lambda_{\mu F(M)}$ and $\lambda = \Lambda_{\mu F(L)}$ where, respectively, stability of the fcc phase is lost and regained under increasing compression; and $\lambda = a$ and $\lambda = b$, where the Gibbs energy for the bcc structure equals that of the fcc structure.

Metal	Stretch (symbolic)	Stretch (numerical)	Pressure (GPa)	Structure of lower Gibbs energy	Structures stable elastically
fcc Cs	Λ_{κ}	1.190	-0.428		
bcc Cs	Λ_{κ}	1.188	-0.432	fcc	
Cs	a	1.048	-0.24		fcc
Cs	b	0.706	14.0	fcc	fcc
bcc Cs	$\Lambda_{\mu B(M)}$	0.681	18.1	bcc	
bcc Cs	$\Lambda_{\mu B(L)}$	0.564	65.4	fcc	fcc
				⋮	⋮
fcc Rb	Λ_{κ}	1.190	-0.575		
bcc Rb	Λ_{κ}	1.188	-0.581	fcc	
Rb	a	1.041	-0.29		fcc
fcc Rb	$\Lambda_{\mu F(M)}$	0.778	8.89	bcc	
fcc Rb	$\Lambda_{\mu F(L)}$	0.700	20.9	fcc	fcc
Rb	b	0.680	25.8		fcc
bcc Rb	$\Lambda_{\mu B(M)}$	0.670	28.8	bcc	
bcc Rb	$\Lambda_{\mu B(L)}$	0.528	140	fcc	fcc
				⋮	⋮
fcc K	Λ_{κ}	1.192	-0.715		
bcc K	Λ_{κ}	1.191	-0.722	fcc	
K	a	1.022	-0.21		fcc
fcc K	$\Lambda_{\mu F(M)}$	0.732	18.6	bcc	
fcc K	$\Lambda_{\mu F(L)}$	0.708	24.1	fcc	fcc
K	b	0.668	37.0		fcc
bcc K	$\Lambda_{\mu B(M)}$	0.653	44.0	bcc	
bcc K	$\Lambda_{\mu B(L)}$	0.520	196	fcc	fcc
				⋮	⋮
fcc Na	Λ_{κ}	1.202	-1.49		
bcc Na	Λ_{κ}	1.201	-1.50	fcc	
Na	a	0.968	0.90		fcc
fcc Na	$\Lambda_{\mu F(M)}$	0.662	87.2	bcc	
fcc Na	$\Lambda_{\mu F(L)}$	0.622	137	fcc	fcc
Na	b	0.600	176		fcc
bcc Na	$\Lambda_{\mu B(M)}$	0.592	192	bcc	
bcc Na	$\Lambda_{\mu B(L)}$	0.458	970	fcc	fcc
				⋮	⋮
fcc Li	$\Lambda_{\kappa F}$	1.216	-2.82		
bcc Li	$\Lambda_{\mu B(R)}$	1.168	-2.77	fcc	
Li	a	0.902	7.31		fcc
fcc Li	$\Lambda_{\mu F(M)}$	0.584	397	bcc	
fcc Li	$\Lambda_{\mu F(L)}$	0.536	731	fcc	fcc
Li	b	0.524	856		fcc
bcc Li	$\Lambda_{\mu B(M)}$	0.522	861	bcc	
				⋮	⋮

shear moduli are positive; thus the zero-pressure bcc and fcc structures both are stable.

(2) The pressure vs stretch curves for the bcc and fcc structures of a given metal are very similar, as are the bulk modulus vs stretch curves for the two structures. In fact,

throughout the ranges of hydrostatic tension and compression that were studied, the difference between the atomic volumes of the bcc and fcc structures of a given metal at any given pressure is less than 0.5%.

(3) In compression, the pressure and bulk modulus both

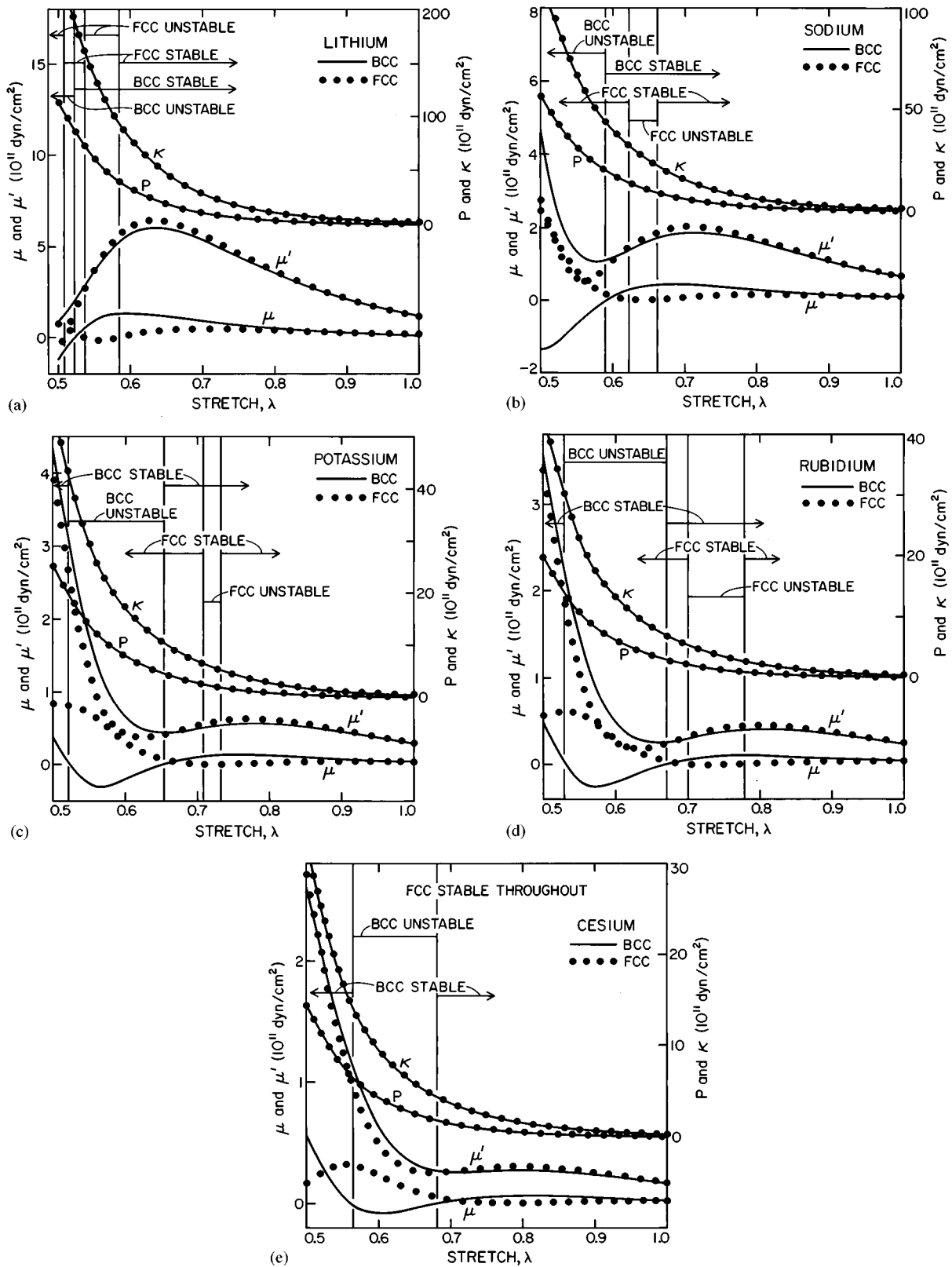


FIG. 1. Pressure and elastic moduli of the bcc and fcc alkali metals in compression; the stretch λ is the lattice parameter divided by its value in the unstressed state ($1 \text{ GPa} = 10^{10} \text{ dyn/cm}^2$).

increase monotonically with decreasing stretch (this was found for all compressive values of stretch, including some values as low as $\lambda = 0.35$). Thus no instabilities of "type (i)" are found in compression.

(4) For both crystal structures, in hydrostatic tension, the bulk modulus decreases, with increasing λ , more rapidly than the shear moduli. For all of the bcc alkalis (except Li) the moduli in tension pass through zero in the order κ, μ, μ' ,

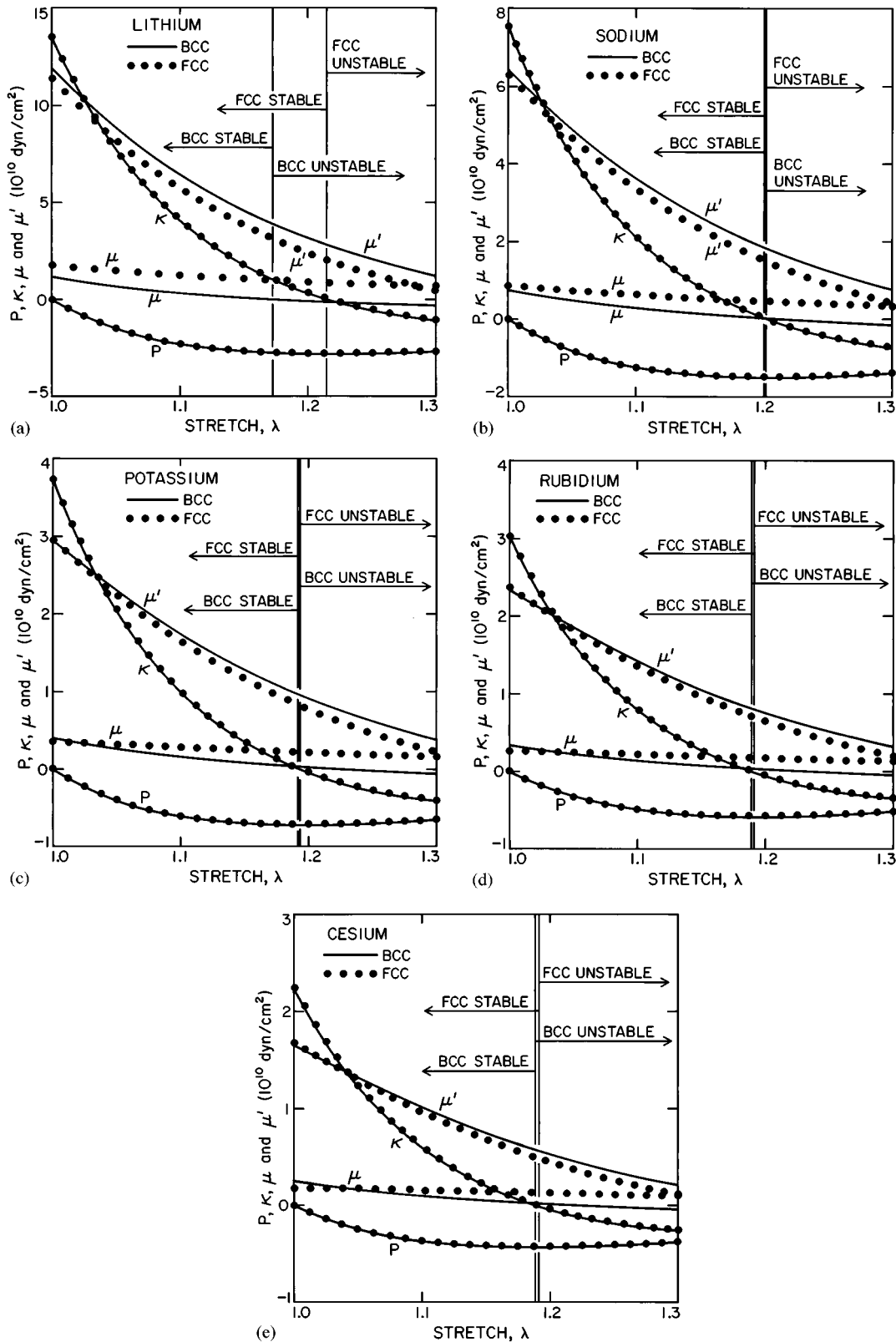


FIG. 2. Pressure and elastic moduli of the bcc and fcc alkali metals in hydrostatic tension ($1 \text{ GPa} = 10^{10} \text{ dyn/cm}^2$).

as λ increases; for the fcc alkalis, the shear moduli approach zero in a more asymptotic manner, and remain positive along the entire tensile range studied (to values of $\lambda = 1.5$). Stability of both the fcc and bcc structures in tension is thus lost when κ passes through zero (and P through a minimum) at $\lambda = \Lambda_{\kappa}$

(except for bcc Li); the values of Λ_{κ} are close to 1.20 and are slightly greater for the fcc than the bcc structure of a given element.

(5) In the neighborhood of $\lambda = 1$, the values of the bcc and fcc shear moduli μ' of a given metal are almost identical;

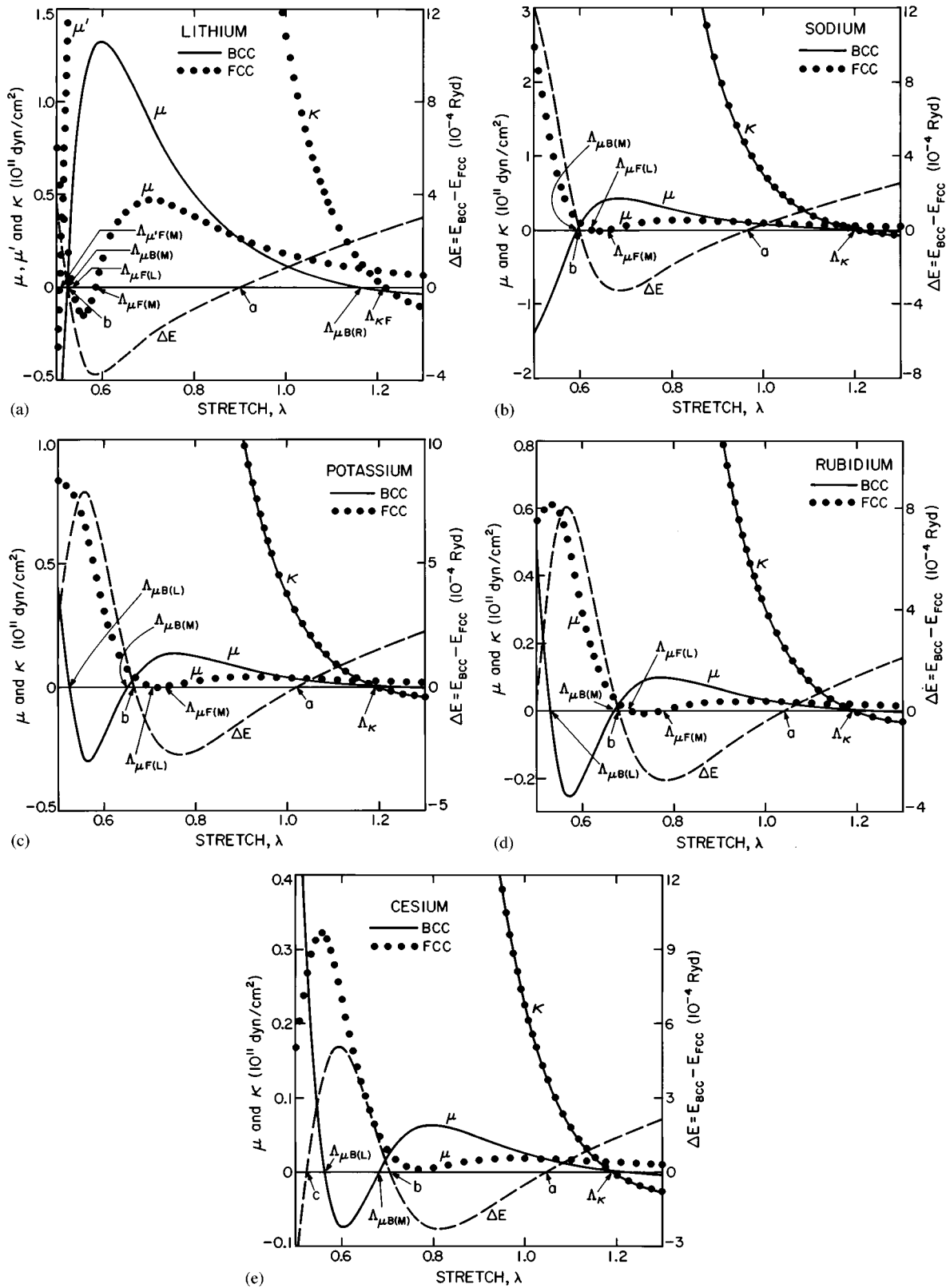


FIG. 3. Gibbs energy difference and elastic moduli that control stability of the bcc and fcc alkali metals in hydrostatic loading; the Λ 's terminate stability ranges (1 GPa = 10^{10} dyn/cm 2). The region of very high compression of (a) is shown in expanded view in Fig. 4.

over the full range of compression and tension, the bcc and fcc functions $\mu'(\lambda)$ behave qualitatively alike. In compression, the functions $\mu'(\lambda)$ exhibit minima (or local minima), but remain positive (fcc Li is an exception); thus (except for

fcc Li under very great compression), there are no instabilities of "type (iii)."

(6) The functions $\mu(\lambda)$ are particularly interesting, not only when considered individually, but as regards the evident

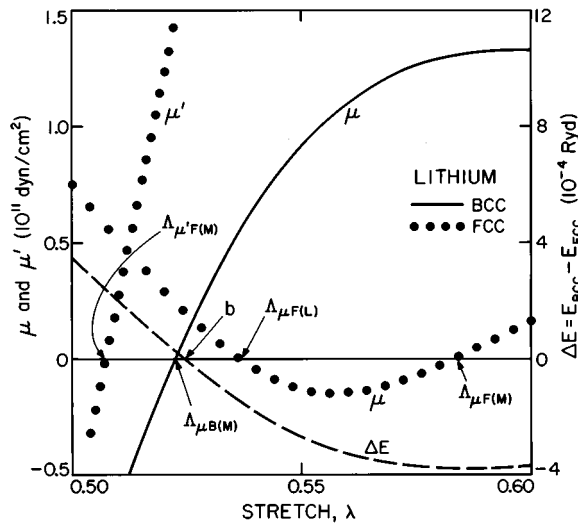


FIG. 4. Expanded view of the theoretical behavior of Li [Fig. 3(a)] under very high compression; it is of interest to note that there is a region ($\lambda < \Lambda_{\mu'_F(M)} = 0.508$) where both μ' of the fcc structure and μ of the bcc structure are negative, and thus both structures are unstable.

“interplay” between the functions $\mu(\lambda)$ of the two considered crystal structures. Although the shear modulus μ of each bcc metal (or μ_B) initially increases with pressure, under continued loading the stable bcc ranges are terminated by instabilities of “type (ii)” at $\lambda = \Lambda_{\mu_B(M)}$, where μ_B becomes negative; another bcc-stable range appears at even greater pressures, where μ_B becomes positive at $\Lambda_{\mu_B(L)}$. [Following the notation of Milstein and Hill^{3,4} the symbols $\Lambda_{\mu_B(L)}$, $\Lambda_{\mu_B(M)}$, and $\Lambda_{\mu_B(R)}$ are used to denote the values of stretch at which the shear modulus $\mu(\lambda)$ of the bcc crystal changes sign algebraically; the subscript B indicates bcc and (L) , (M) , and (R) refer to the left-hand, middle, and right-hand zeros, respectively, in $\mu(\lambda)$; analogous notation applies to the fcc structure.] The fcc shear moduli μ_F tend to be small or negative in regions where μ_B is large and positive; and vice versa. In the metals Li, Na, K, and Rb, stable fcc ranges initially are terminated in compression, by “type-(ii)” instabilities at $\lambda = \Lambda_{\mu'_F(M)}$, and subsequently reappear, under increased pressure, at $\lambda = \Lambda_{\mu'_F(L)}$, yielding an intermediate unstable fcc range. In Cs, μ_F becomes small, indicating “weak stability” of the fcc configuration, in the analogous region of stretch.

Since the variations of pressure with stretch for the fcc and bcc phases are almost identical, the difference in Gibbs energy ΔE of the two phases at a given pressure may be represented on a plot where the stretch λ is the independent variable, as shown in Figs. 3(a)–3(e) and 4. For practical purposes, the Gibbs energy differences are the differences in binding energies per atom, since the pressure-volume products are almost identical at a given pressure or volume. For each of the alkali metals, at relatively large values of stretch (i.e., $\lambda > a$ in Figs. 3) ΔE is positive, so the fcc, or close-packed, phase is favored thermodynamically, when compared with bcc; over a broad intermediate range ($b < \lambda < a$) ΔE is negative, favoring bcc; at still greater compressions, ΔE again becomes positive at $\lambda = b$, and thus fcc again becomes the preferred phase (where $\lambda < b$). In passing through

the series from Cs to Li, the states where $\lambda = a$, $\lambda = b$, and $\lambda = \Lambda_{\mu_B(M)}$ are seen to occur at progressively lower values of stretch; i.e., through this series, the curves $\mu(\lambda)$ and $\Delta E(\lambda)$ are shifted toward the region of higher compression. It is particularly interesting to note that the states “ $\lambda = a$,” where the Gibbs energy difference vanishes (in Figs. 3), occur in regions of hydrostatic tension for K, Rb, and Cs and in compression for Na and Li. Thus, although both the bcc and fcc phases of all five alkali metals are elastically stable at zero pressure, the thermodynamically preferred zero-pressure structures (i.e., the structures with the lower Gibbs energy) at low temperatures are indicated to be bcc for K, Rb, and Cs and fcc for Li and Na, in good agreement with experiment (i.e., the low-temperature phases of K, Rb, and Cs are indeed bcc while Li and Na are closed packed similar to “faulted fcc”).

Figures 3 also display the critical role of the shear modulus μ and the interplay between μ and the Gibbs energy difference ΔE . At $\lambda = a$ and at $\lambda = b$, where both phases have the same Gibbs energy and are equally favored thermodynamically, the values of μ_B and μ_F are very close. Where μ_B is substantially greater than μ_F , ΔE is strongly negative, favoring the bcc structure; and vice versa where μ_F is considerably larger than μ_B . Often the literature fails to distinguish between issues of “stability” and “thermodynamically preferred phase;” the present results help clarify these concepts. Consider, e.g., the bcc phase of Rb to be compressed to a state where $\Lambda_{\mu_B(M)} < \lambda < b$, i.e., to where $0.670 < \lambda < 0.680$ for the present computational model. Here the fcc structure has a lower Gibbs energy, but the bcc crystal is still elastically stable; it would take some “finite disturbance,” to cause a transformation from the bcc to the fcc state. In principle, in the absence of disturbance, the metal could remain in the elastically stable but thermodynamically disfavored bcc structure; the closer the system is to the state where $\lambda = \Lambda_{\mu_B(M)}$, the smaller the disturbance required to cause the transition; at $\lambda = \Lambda_{\mu_B(M)}$, an infinitesimal disturbance would trigger the transformation. (In an imperfect crystal, i.e., an actual metal crystal, “internal disturbances” of some magnitude of course are unavoidable owing to localized stress raisers associated with defects.)

In the cases of K, Rb, and Cs, theoretically the stable bcc structure thus transforms to fcc at compressions in the range $\Lambda_{\mu_B(M)} < \lambda < b$, with the transformation pressure greatest for K and least for Cs, in good agreement with experiment.⁵ (Our calculations, suggesting a bcc to fcc transformation in K under pressure, were in fact carried out before this was observed experimentally.) The computations also show the transitions to be associated with instabilities of type (ii). Further, there is experimental evidence that these fcc metals again transform to other structures, at still higher pressures; not all of these have been identified, although some may be tetragonal and/or have eight nearest-neighbor atoms.⁵ Accordingly, the theoretical shear moduli μ of these fcc metals under increasing pressure again vanish, suggesting such further transformations. Our computed transformation pressures (and volumes) for these metals are somewhat greater (and smaller) than experiments would suggest. For example, experimentally the bcc→fcc transitions in K, Rb, and Cs are observed at pressures ranging from about 2 GPa (for Cs) to 11 GPa (for K),⁵ whereas theoretically the Gibbs energy dif-

ference vanishes (at $\lambda=b$) at pressures ranging from 14 to 37 GPa for these metals. This is within the range of other computations, which have suggested corresponding theoretical transformation pressures as high as about 50 GPa for K and Rb.⁵ The numerical discrepancy between theory and experiment may be variously explained. For example, Milstein *et al.*¹⁹ have pointed out one possible source of discrepancy, which may result from experimental technique, i.e., from nonhydrostatic components of stress which may be present in a high-pressure test. In particular, they used the present pseudopotential model to study the stability of the alkali metals under uniaxial loading and found that bcc→fcc transitions occur under both uniaxial tensile and uniaxial compressive stresses, and the magnitudes of the uniaxial stresses required to initiate the transitions in K, Rb, and Cs are close to 2 orders of magnitude less than the “hydrostatic” pressures at which the transitions are observed. This suggests¹⁹ “that the combined effect of a relatively small uniaxial component of stress “superimposed” on a large hydrostatic compression could cause a bcc→fcc transition well before it would occur in the absence of the uniaxial component.”

In view of the above consideration, the qualitative agreement between theory and experiment is considered excellent and the quantitative agreement, “reasonably good.” However, another possible source of the numerical discrepancy between the calculated and observed bcc→fcc transition pressures in the heavier alkali metals may be that the pseudopotential model does not fully account for repulsion between core electrons under very high pressures. As a first approximation, *d*-band overlap in simple metals may be represented by Born-Mayer (BM) repulsive interactions,^{20–22} i.e., by adding an overlap energy term of the form

$$\frac{1}{2} \sum_r A \exp \left[-B \left(\frac{r}{r_n} - 1 \right) \right]$$

to the binding energy, where *A* and *B* are positive constants and r_n is the nearest-neighbor distance in the unstressed bcc configuration. This overlap energy term was included in the present study for selected computations with Cs and Rb. It was found that, for appropriate choices of the parameters *A* and *B*, the theoretical values of $\Lambda_{\mu_B(M)}$ and *b* can be increased considerably (without changing appreciably the computed low-pressure behavior), to bring them more in line with what would be expected experimentally (the results in Figs. 1–4 were computed without this interaction). For example, with the inclusion of BM interactions for the cases of $A=0.75 \times 10^{-5}$ Ry for Rb and $A=2.2 \times 10^{-5}$ Ry for the Cs, with $B=20$ (for both Cs and Rb), the Gibbs energies of the bcc and fcc phases become equal at $\lambda=b=0.856$ for Cs and $\lambda=b=0.778$ for Rb, with the corresponding pressures at these points equal to 2.7 GPa for Cs and 9.6 GPa for Rb; the bcc structures then become unstable at $\Lambda_{\mu_B(M)}=0.774$ for Cs and $\Lambda_{\mu_B(M)}=0.718$ for Rb, with corresponding pressures of 8.5 and 20.5 GPa, respectively. The Born-Mayer interactions were introduced without altering the pseudopotential parameters; the effect of these interactions on various unstressed properties (i.e., at $\lambda=1$) of the bcc structure is seen from the following list, which is in the format [property: value for Cs without the BM interactions, value for Cs with the BM interactions; value for Rb without . . . , . . . Rb with . . .].

[E_{bind} in Ry: $-0.344, -0.344; -0.368, -0.368$], [lattice parameter in Bohr radii: 11.4205, 11.4399; 10.5388, 10.5441], [κ in GPa: 22.4, 23.2; 30.2, 30.5], [μ in GPa: 2.47, 2.40; 3.34, 3.31], [μ' in GPa: 16.6, 17.2; 23.4, 23.7], [$d\kappa/dP$: 3.72, 3.85; 3.77, 3.81], [$d\mu/dP$: 0.271, 0.241; 0.268, 0.258], [$d\mu'/dP$: 1.07, 1.24; 1.16, 1.21], [$d^2\kappa/dP^2$ in (GPa)⁻¹: $-1.9, -1.6; -1.3, -1.2$], [$d^2\mu/dP^2$ in (GPa)⁻¹: $-0.33, -0.34; -0.23, -0.23$], and [$d^2\mu'/dP^2$ in (GPa)⁻¹: $-1.7, -1.4; -1.3, -1.3$] (corresponding experimental values are listed in Tables I and II of Ref. 1).

Also, our theoretical results are in good agreement with the experimental observation that Na transforms from the close-packed structure to bcc at a relatively low pressure, with the bcc and close-packed structures coexisting over a large range of pressure.^{5,6} That is, the Gibbs energies of the bcc and fcc structures of Na become equal (at $\lambda=a$) at a relatively small pressure, although here the transformation does not seem to be associated with the vanishing of a shear modulus, since both μ_B and μ_F are appreciably large and positive at state *a*, and remain so over large ranges of compression. This “strong” elastic stability of both phases is thus also consistent with the observed “coexistence” of the two apparently stable phases. As in the case of the higher pressure bcc→fcc transformations in Cs, Rb, and K, the indicated theoretical transformation pressure in Na is somewhat greater than what experiment would suggest; i.e., at low temperature, Na is found to transform to bcc in the range 0.1–0.2 GPa,⁵ whereas the state “ $\lambda=a$ ” resides at about 0.90 GPa in the pseudopotential model of Na. A further bcc→fcc transition in Na is suggested at very high pressures, but has not, as yet, been observed. According to the model computations, Li also undergoes a close-packed→bcc transition that is “sluggish” and this occurs at greater pressures than those at which the analogous transition occurs in Na. Experimentally, Li is thought to undergo a crystallographic phase change at 7 K and 26 GPa, based on resistance curves.⁵ Since the points where $\lambda=a$ occur where $\lambda>1$ in K, Rb, and Cs, these metals would also be expected to undergo similar “sluggish” transformations from bcc to close packed, but in regions of hydrostatic tension. It is noteworthy (and perhaps contrary to one’s intuition) that *increasing compression* stabilizes the bcc structure (which is usually thought of as “more open”) at the expense of fcc; this increasing stabilization of bcc occurs over large ranges of tension and compression (i.e., where the slope of ΔE is positive in Figs. 3).

There are few studies (of the behavior of the bulk and shear moduli of metals under pressure) with which the present work may be compared, although other investigators have reported “shear modulus instabilities” in silicon²³ and in α quartz²⁴ under pressure. The earlier work with Morse functions^{3,4} did not exhibit transitions from stability to instability under increasing compression, although there are some remarkable similarities among the mechanical behaviors of the Morse function crystals and the pseudopotential model crystals. For example, the Morse model bcc shear moduli $\mu_B(\lambda)$ were found to be negative throughout an intermediate range of stretch values, and positive under both large compressions (small λ) and large expansions (large λ), not unlike the present functions $\mu_B(\lambda)$. However, in the Morse model computations, the ranges of negative values of $\mu_B(\lambda)$ either

were entirely in the region of tension, i.e. $\lambda > 1$ (in which cases the bcc crystals were stable at $\lambda = 1$ and did not become unstable under compression) or the “negative ranges” included the zero-pressure state at $\lambda = 1$ (then the bcc crystals were unstable at $\lambda = 1$, but eventually became stable under increasing pressure). The characteristic behavior of the Morse model bcc and fcc crystals depended on the “range parameter,” $\ln\beta$; for a given value of $\ln\beta$, the P vs λ and κ vs λ curves were almost identical for the bcc and fcc structures, as in the present study. Values of $\ln\beta \approx 2.9-3.3$ model the zero-pressure elastic properties and the pressure volume behavior of the alkali metals fairly well (see Figs. 7 and 8 of Ref. 1). For example, the ratio of the shear moduli μ/μ' for bcc Morse model crystals at zero pressure varies from about 0.1 (for $\ln\beta = 3.3$) to 0.14 (for $\ln\beta = 2.9$); the experimental range is also about 0.1 (for Li) to 0.14 (for K). Also, for this range of values of $\ln\beta$, the bcc moduli are all positive initially, and in tension they pass through zero in the order κ , μ , μ' as λ increases, with κ vanishing at $\lambda \approx 1.2$, in excellent agreement with the behavior of the alkali metals in the pseudopotential model. For Li, which has the smallest zero-pressure shear moduli ratio, μ passes through zero before κ in the pseudopotential computations under tension; here again there is qualitative agreement with the Morse model;

i.e., for Morse model bcc crystals with small shear moduli ratios (specifically, $\mu/\mu' \leq 0.05$, which occurs when $\ln\beta \geq 3.91$), $\mu(\lambda)$ becomes negative before $\kappa(\lambda)$ as λ increases, in tension.

Finally, we mention an additional theoretical study²⁵ that deals with post-bifurcation phenomena. First-order bifurcation theory (i.e., inclusive of the second-order elastic moduli) predicts that the homogeneous eigenmode (associated with loss of stability when $\kappa > 0$, $\mu' > 0$, and $\mu = 0$) makes the lattice orthorhombic with no variation of volume,^{2,3} i.e., the initial departure of a previously stable cubic cell of edges $a_1 = a_2 = a_3$ from its primary equilibrium path is given by $\delta a_1 + \delta a_2 + \delta a_3 = 0$, with cell edges remaining mutually orthogonal. In the forthcoming work, (i) it is found that equilibrium *tetragonal* paths, under hydrostatic pressure, link the respective cubic paths at the states where $\mu_B = 0$ and $\mu_F = 0$; (ii) a general relation derived among third order moduli at the branch point proves that homogeneous branching of a cubic crystal under hydrostatic loading at $\mu = 0$ must be from cubic to tetragonal; (iii) calculations of the third-order moduli at $\mu = 0$ verify this relation. This is important owing to the possible existence of tetragonal phases in some of the alkali metals under very high pressures.⁵

*Present address: NASA-AMES Research Center, Moffett Field, California 94035-1000.

¹D. J. Rasky and F. Milstein, *Phys. Rev. B* **33**, 2765 (1986).

²R. Hill and F. Milstein, *Phys. Rev. B* **15**, 3087 (1977).

³F. Milstein and R. Hill, *J. Mech. Phys. Solids* **27**, 255 (1979).

⁴F. Milstein and R. Hill, *Phys. Rev. Lett.* **43**, 1141 (1979).

⁵D. A. Young, *Phase Diagrams of the Elements* (University of California Press, Berkeley, 1991).

⁶H. G. Smith, R. Berliner, J. D. Jorgensen, and J. Trivisonno, *Phys. Rev. B* **43**, 4524 (1991).

⁷R. Hill, in *Advances in Applied Mechanics*, edited by C.-S. Yih (Academic, New York, 1978), Vol. 18, p. 1.

⁸F. Milstein, *Phys. Rev. B* **3**, 1130 (1971).

⁹N. H. Macmillan and A. Kelly, *Proc. R. Soc. London, Ser A* **330**, 309 (1972).

¹⁰J. Wang, S. Yip, S. Phillpot, and D. Wolf, *J. Alloys Comp.* **194**, 407 (1993).

¹¹M. Born, *Proc. Cambridge Philos. Soc.* **36**, 160 (1940).

¹²M. Born and R. Fürth, *Proc. Cambridge Philos. Soc.* **36**, 454 (1940).

¹³R. Fürth, *Proc. Cambridge Philos. Soc.* **37**, 177 (1941).

¹⁴R. Hill, *Math. Proc. Cambridge Philos. Soc.* **77**, 225 (1975).

¹⁵D. C. Wallace, *Thermodynamics of Crystals* (Wiley, New York, 1972).

¹⁶V. Heine and D. Weaire, in *Solid State Physics*, edited by H. Ehrenreich, F. Seitz, and D. Turnbull (Academic, New York, 1970), Vol. 24.

¹⁷R. Taylor, *J. Phys. F* **8**, 1699 (1978).

¹⁸D. Sen and S. K. Sarkar, *Phys. Rev. B* **22**, 1856 (1979).

¹⁹F. Milstein, J. Marschall, and H. E. Fang, *Phys. Rev. Lett.* **74**, 2977 (1995).

²⁰J. A. Moriarty, *Phys. Rev. B* **6**, 1239 (1972).

²¹J. F. Thomas, Jr., *Phys. Rev. B* **7**, 2385 (1973).

²²F. Milstein and D. J. Rasky, *Phys. Rev. B* **33**, 2341 (1986).

²³K. Mizushima, S. Yip, and E. Kaxiras, *Phys. Rev. B* **50**, 14952 (1994).

²⁴N. Binggeli and J. R. Chelikowski, *Phys. Rev. Lett.* **69**, 2220 (1992).

²⁵F. Milstein, H. E. Fang, X.-Y. Gong, and D. J. Rasky, *Solid State Commun.* (to be published).